

Scaling in local to global condensation of wealth on sparse networks

Hyun Gyu Lee^{1,*} and Deok-Sun Lee^{1,2,†}

¹*School of Computational Sciences, Korea Institute for Advanced Study, Seoul 02455, Korea*

²*Center for AI and Natural Sciences, Korea Institute for Advanced Study, Seoul 02455, Korea*

(Dated: July 31, 2023)

The prevalence of wealth inequality propels us to characterize its origin and progression, via empirical and theoretical studies. The Yard-Sale(YS) model, in which a portion of the smaller wealth is transferred between two individuals, culminates in the concentration of wealth to a single individual, while distributing rest of the wealth with a power-law of exponent one. By incorporating redistribution to the model, in which the transferred wealth is proportional to the sender's wealth, we show that such extreme inequality is suppressed if the redistribution occurs more frequently than the inverse of the population size. Studying our model on a sparsely-connected population, we find that the wealth inequality ceases to grow for a period, when local rich nodes can no longer acquire wealth from their broke nearest neighbors. Subsequently, inequality resumes growth due to the redistribution effect by allowing locally amassed wealth to move and coalesce. Analyzing the Langevin equations and the coalescing random walk on complex networks, we elucidate the scaling behaviors of wealth inequality in those multiple phases. These findings reveal the influence of network structure on wealth distribution, offering a novel perspective on wealth inequality.

Wealth inequality may be attributed to a myriad of socioeconomic factors and their orchestration. Yet the universal power-law wealth and income distributions [1–3] imply a common mechanism at play, and provide the possibility of theoretical understanding on how wealth inequality has arisen and how long it will persist [4–6]. Grounded on the idea that individuals participating in a trade can undergo wealth transfer due to imperfect pricing, various computational models of wealth exchange have been studied extensively, and their steady-state solutions, often available analytically, serve as plausible explanations for various wealth distributions [7–13].

The Yard-Sale(YS) model [14, 15] is remarkable as it generates an extreme wealth inequality from a seemingly fair (and thus realistic) exchange rule: A fraction of the sender's and receiver's smaller wealth is transferred in each trade, and ultimately, almost total wealth is concentrated in a single individual while the remaining wealth being distributed by a power-law with exponent one across the rest of the population [16]. The model's simplicity and yet the emergence of such stark inequality have attracted much attention [16–22]. However, such global wealth condensation does not (yet) happen in the real world, undermining the reality of the long-time-limit solution.

The degree of real-world wealth inequality has been changing with time [4–6]. In this light, the non-stationary state, rather than the stationary state, of a model may offer a better explanation of the reality. Also, by relaxing constraints like the fully-connected population often assumed in many studies and by considering multiple modes of wealth exchange, the YS model can become more realistic and reveal a richer set of insights. For example, wealth transfer equal to a fraction of the sender's wealth, occurring in donation, investment, or taxation, effectively redistributes wealth and

suppresses wealth inequality [7–9, 18]. Investigating the non-stationary state of the generalized YS model [16, 22] which allows such redistribution (RD) mode of wealth transfer, as well as the YS-mode, between connected pairs in a structured population [21], we identify new relevant factors influencing wealth inequality and provide a novel theoretical framework.

We show that the extreme inequality of the original YS model in the long-time limit can be suppressed by increasing the ratio of the RD-mode transfers beyond the inverse of the population size. In the sparsely-connected population, inequality evolves with time through multiple phases, and we elucidate the underlying mechanisms. Initially, the inequality grows primarily driven by the YS-mode wealth transfer before saturating over a period of time due to depleted wealth of the nearest neighbors of locally rich nodes. We call this stage *local condensate* phase. As time passes, the RD-mode transfer effectively thaws this frozen state, enabling further elevation of inequality via processes akin to random walk and coalescence of locally-concentrated wealth. In these stages, scaling behaviors of wealth inequality emerge, and we show that they originate from intimate relationships between the dynamics of wealth and the network structure. This demonstrates the critical role of the structure of networks in understanding the wealth distribution. Finally, comparing with the empirical data, we discuss the implications of our findings.

Model – We consider a network of N nodes (individuals) connected by L undirected links (trade partnership) with the adjacency matrix $A_{ij} = 0, 1$. Each node i has wealth $\omega_i(t)$ with $\omega_i(t = 0) = 1$ initially. For every pair of connected nodes with rate N/L , the sender ('s') and the receiver ('r') are determined randomly and the sender sends an amount $\Delta\omega$ of wealth to the receiver [Fig. 1 (a)],

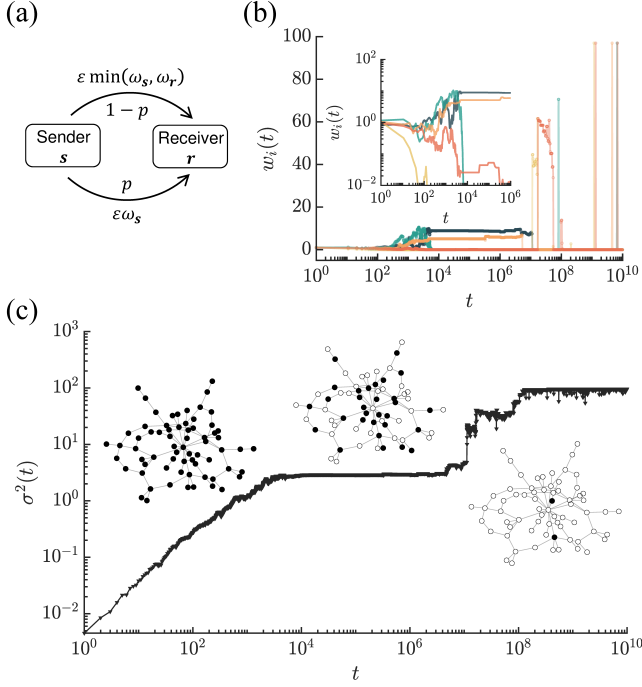


Figure 1. Model and its Monte-Carlo simulation results. (a) Two modes of wealth transfers in Eq. (1). (b) Time-evolution of individual wealth in a single run of the Monte-Carlo simulation with $p = 10^{-6}$ and $\varepsilon = 0.05$ on a SF network of $N = 97$ nodes, $L = 200$ links and the degree exponent $\gamma = 2.5$. Inset: The same plots for $1 \leq t \leq 10^6$. (c) Time-evolution of wealth variance from the same simulation. Three insets represent a part of the network at $t = 10^2$, 10^5 , and 10^{10} , respectively, with rich (poor) nodes colored black (white).

where $\Delta\omega$ is a fraction ε of either the smaller wealth or the sender's wealth as

$$\Delta\omega = \begin{cases} \varepsilon \min\{\omega_s, \omega_r\} & \text{with prob. } 1-p \text{ (YS mode),} \\ \varepsilon \omega_s & \text{with prob. } p \text{ (RD mode).} \end{cases} \quad (1)$$

Consequently their wealth change as $(\omega_s, \omega_r) \rightarrow (\omega_s - \Delta\omega, \omega_r + \Delta\omega)$, but their sum is preserved. The mean wealth is fixed, i.e., $\bar{\omega} = N^{-1} \sum_i \omega_i(t) = 1$. The probability p is the relative ratio of the RD-mode transfers. This is a network version of the model introduced in Refs. [16, 22]. For the underlying networks, we use the complete graphs ($A_{ij} = 1$ for all $i \neq j$) and the giant connected components of sparse scale-free (SF) networks [23] constructed by the static model [24, 25], which display power-law degree distributions $P_{\text{deg}}(k) \equiv N^{-1} \sum_i \delta_{k_i, k} \sim k^{-\gamma}$ for large k with the degree $k_i = \sum_j A_{ij}$ meaning the number of the nearest neighbors and γ called the degree exponent, and have the mean degree $\bar{k} = 2L/N$ finite.

For a measure of wealth inequality we use the wealth variance

$$\sigma^2(t) \equiv \frac{1}{N} \sum_{i=1}^N (\omega_i(t) - \bar{\omega})^2,$$

which is the second cumulant of the wealth distribution $P(\omega, t)$. A single run result of the model simulation with small p readily reveals multiple phases in the time-evolution of wealth inequality. See Figs. 1(b) and 1(c). i) For $t \lesssim 10^4$, individuals' wealth is made increasingly different from one another, resulting in the growth of wealth inequality. ii) Then a frozen period follows ($10^4 \lesssim t \lesssim 10^7$), when ω_i 's and σ^2 hardly change with time. *Rich* nodes, possessing wealth larger than the average ($\omega_i \geq \bar{\omega} = 1$), are surrounded by the *poor* nearest neighbors ($\omega_j < 1$). With $p = 0$, this local condensate phase becomes the equilibrium as shown in Fig. S1 in Supplemental Material (SM) [26] and also reported in Ref. [21]. iii) In the late-time regime ($10^7 \lesssim t \lesssim 10^8$), the wealth variance resumes growing and the locally-concentrated wealth switches its host node to one of its nearest neighbors repeatedly, appearing to perform a random walk, until it encounters another local wealth and they coalesce [27]. iv) Very late ($t \gtrsim 10^8$), global condensation occurs; almost all wealth is concentrated onto a single node. Yet its host changes with time and σ^2 fluctuates though weakly.

Langevin equation— To understand these observations quantitatively and proceed, we consider the Langevin equation of the model

$$d\omega_i = -\frac{\varepsilon p}{\bar{k}} \sum_j L_{ij} \omega_j dt + \varepsilon \sqrt{2p D^{(\text{RD})}(\omega_i)} dX_i + \varepsilon \sqrt{2(1-p) D^{(\text{YS})}(\omega_i)} dY_i, \quad (2)$$

where $L_{ij} \equiv k_i \delta_{ij} - A_{ij}$ is the Laplacian, dX_i and dY_i are the Wiener processes with mean 0 and variance dt representing the stochasticity of whether to send or receive wealth, and the coefficients $D^{(\text{RD})}(\omega_i) = \langle \{(\omega_i + \omega)/2\}^2 \rangle$ and $D^{(\text{YS})}(\omega_i) = \langle \min\{\omega_i, \omega\}^2 \rangle$ are the mean square of the transferred wealth for node i under the RD and YS mode, respectively, with $\langle \dots \rangle$ denoting the ensemble average. The first and second terms represent the deterministic and stochastic changes by the RD-mode transfers, and the third one from the YS transfers. The derivation of Eq. (2) is in SM.

In the early-time regime, ω_i 's remain close to the initial value, and thus $D^{(\text{YS})}(\omega_i) \simeq D^{(\text{RD})}(\omega_i) \simeq 1$, which leads to the approximation $d\omega_i \simeq \sqrt{2}\varepsilon dY_i$ and $d\omega_i \simeq \sqrt{2}\varepsilon dX_i$ for small and large p , respectively. Therefore, as shown in Figs. 2(a), 3(a), and S2, we find

$$\sigma^2(t) \simeq 2\varepsilon^2 t. \quad (3)$$

This linear growth cannot continue indefinitely for finite N but σ^2 eventually saturates. The equilibrium value varies with the ratio p of the RD mode as [Fig. 2(b)]

$$\sigma_{\text{eq}}^2 \equiv \lim_{t \rightarrow \infty} \sigma^2(t) \sim \begin{cases} N & \text{for } p \ll p_* \equiv \frac{\varepsilon}{N}, \\ \frac{\varepsilon}{p} & \text{for } p \gg p_*. \end{cases} \quad (4)$$

The critical ratio p_* and Eq. (4) can be obtained as follows. For $p = 0$ or small p , the model is similar to the original YS model and almost all wealth is concentrated in a single node in the long-time limit [16] yielding $\sigma_{\text{eq}}^2 \simeq N$. For p relatively large, let us use the approximation $\sum_j L_{ij}\omega_j \simeq \bar{k}(\omega_i - 1)$, which is the mean-field approach that becomes exact in the complete graph. In equilibrium, the fluctuation driven by the YS-mode transfers $(\delta\omega)_{\text{YS}} \sim \varepsilon\sqrt{2t_{\text{eq}}D_{\text{YS}}}$ is balanced by the redistribution $(\delta\omega)_{\text{RD}} \sim \varepsilon p(\delta\omega)_{\text{YS}}t_{\text{eq}}$ in a time interval t_{eq} , which allows us to estimate $t_{\text{eq}} \sim \frac{1}{\varepsilon p}$ and $\sigma_{\text{eq}}^2 \sim (\delta\omega)_{\text{YS}}^2 \sim (\delta\omega)_{\text{RD}}^2 \sim \frac{\varepsilon}{p}$. It is the fluid phase of wealth. The two values of σ_{eq}^2 become comparable at the threshold $p_* \equiv \frac{\varepsilon}{N}$. Simulations on the complete graphs support Eq. (4) [Fig. 2(b)]. The equilibration time t_{eq} when $\sigma^2(t)$ following Eq. (3) reaches σ_{eq}^2 is given by $t_{\text{eq}} \sim \frac{N}{\varepsilon^2}$ for $p \ll \frac{\varepsilon}{N}$, and $t_{\text{eq}} \sim \frac{1}{\varepsilon p}$ for $p \gg \frac{\varepsilon}{N}$ [Fig. S2].

The wealth distribution $P(\omega, t)$ is available, though partially, in the mean-field approach. With a low ratio of the RD-mode transfers ($p \ll p_*$), the Fokker-Planck (FP) equation is approximated as $\partial P/\partial t \simeq \varepsilon^2(\partial^2/\partial\omega^2)\{D^{(\text{YS})}(\omega)P\}$. Recalling $D^{(\text{YS})}(\omega) \simeq \omega^2$ for $\omega \ll 1$ and $D_{\text{YS}}(\omega) \simeq 1$ for $\omega \gg 1$ in the early-time regime, we obtain [26]

$$P(\omega, t) \simeq \begin{cases} \frac{e^{-\frac{t\varepsilon^2}{4}}}{\sqrt{4\pi\varepsilon^2 t}\omega^{3/2}} \exp\left[-\frac{(\log\omega)^2}{4\varepsilon^2 t}\right] & \text{for } \omega \ll 1, \\ \frac{1}{\sqrt{4\pi\varepsilon^2 t}} e^{-\frac{(\omega-1)^2}{4\varepsilon^2 t}} & \text{for } \omega \gg 1, \end{cases} \quad (5)$$

in agreement with the simulation results [Fig. 2(b)]. Note that the width of these distributions is commonly given by $\langle\omega^2\rangle - 1 \simeq 2\varepsilon^2 t$ for $\varepsilon^2 t \ll 1$ in agreement with Eq. (3). In the long-time limit, a node occupies almost all wealth and the rest shows a power-law distribution $P(\omega, t) \sim \frac{1}{\varepsilon^2 t \omega}$ [Fig. S3] as obtained by solving the Boltzmann equation [16, 26].

With $p \gg p_*$, one can approximate Eq. (2) as $d\omega \simeq -\varepsilon p(\omega - 1)dt + \varepsilon\sqrt{2(1-p)}\omega dY$ for small ω . This Langevin equation has been studied as a model for power-law wealth distributions [8] and also for the stationary state of the YS model with redistribution [16, 22]; The stationary-state solution to the corresponding FP equation is the inverse gamma distribution [26]

$$P_{\text{eq}}(\omega) \simeq \frac{\mu^{\mu+1}}{\Gamma(\mu+1)} \omega^{-2-\mu} e^{-\frac{\mu}{\omega}}, \quad (7)$$

where $\mu \equiv \frac{p}{\varepsilon(1-p)} \simeq \frac{p}{\varepsilon}$ and the width is $\langle\omega^2\rangle - 1 = \frac{1}{\mu-1} \simeq \frac{\varepsilon}{p}$ for large μ . Note that it is a power-law $P_{\text{eq}}(\omega) \sim \omega^{-2-\frac{p}{\varepsilon}}$ for large ω [8] while Eq. (7) here describes only the small- ω behavior of our model.

Local condensate phase— For sparse networks, the early- and stationary-state behaviors remain similar to those

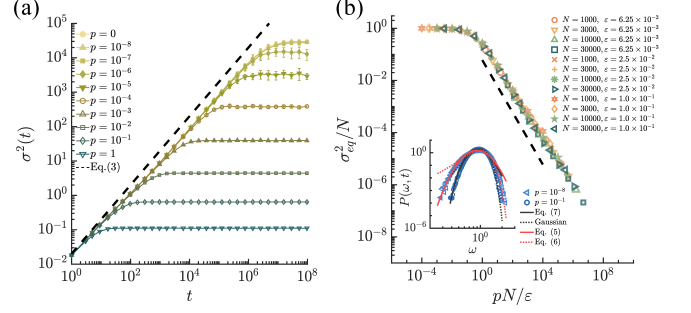


Figure 2. Wealth variance and distribution on the complete graphs. (a) Wealth variance for $\varepsilon = 0.1$ and different p 's on the complete graph with $N = 10^5$ averaged over 20 realizations. (b) Data collapse of the rescaled wealth variance in the equilibrium state for different p 's, ε 's and N 's. The dashed line has slope -1 . Inset: Wealth distributions for $\varepsilon = 0.00625$, $N = 10^5$, and different p 's at time $t = 10^3$. Lines represent the analytic predictions. ‘Gaussian’ denotes

$$P(\omega, t) = \frac{1}{\sqrt{2\pi\sigma^2(t)}} e^{-\frac{(\omega-1)^2}{2\sigma^2(t)}}.$$

on the complete graphs given in Eqs. (3) and (4). See Fig. 3(a). However, in the intermediate-time regime $t_{\text{lc}} \lesssim t \lesssim t_{\text{rel}}$, the wealth variance ceases to grow but remains fixed. Setting the ratio of RD transfers to be small, we here investigate the novel phases emerging on sparse networks.

The fixed value of wealth variance in this local condensate phase is related to the sparse connection of the underlying network. Each rich node i is found to have taken almost all the wealth of its nearest neighbors, possessing $\omega_{i,\text{rich}} \simeq k_i + 1$ including its own as well [Fig. 3(b)]. Hub nodes thus possess more as long as they are rich. Yet the probability of a node i to be rich decreases with its degree as $\rho_{i,\text{rich}} \simeq \frac{1}{k_i+1}$ [Fig. 3(c)], for a node and its neighbor(s) are equally likely to be rich under the YS-mode transfer.

Introducing the wealth $\omega_{\text{rich}}(k)$ of a rich node of degree k and the probability $\rho_{\text{rich}}(k)$ of a node of degree k to be rich and approximating the wealth of a poor node to be zero, one can represent the wealth variance as

$$\sigma^2 \simeq \sum_k P_{\text{deg}}(k) \left[\rho_{\text{rich}}(k) \{\omega_{\text{rich}}(k) - 1\}^2 + 1 - \rho_{\text{rich}}(k) \right]. \quad (8)$$

Using $\rho_{\text{rich}}(k) \simeq 1/(k+1)$ and $\omega_{\text{rich}} \simeq k+1$, we obtain

$$\sigma^2 \simeq \bar{k}, \quad (9)$$

which is supported by Figs. 3(e) and (f). Recalling the initial growth of the wealth variance in Eq. (3), we find local condensation begins at $t_{\text{lc}} \sim \frac{\bar{k}}{\varepsilon^2}$, which can be rationalized by considering that it takes time ε^{-2} for a node to take the wealth of a neighbor by the YS-mode transfers, and it has \bar{k} such neighbors on the average. Local condensation is terminated at t_{rel} , when the RD-mode transfers begin to redistribute significantly

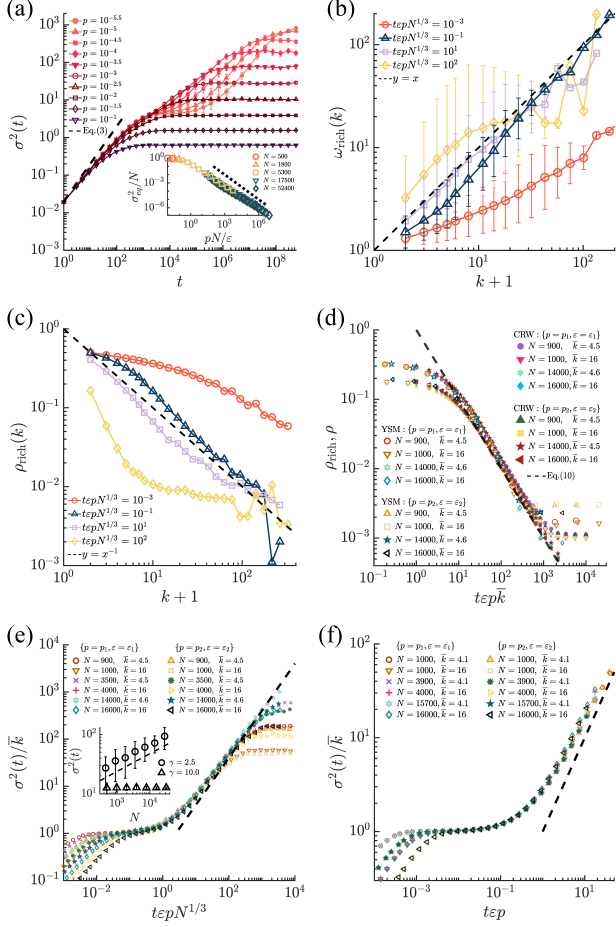


Figure 3. Scaling of wealth variance on SF networks. (a) Wealth variance for $\varepsilon = 0.1$ and different p 's on SF networks with $N = 887 \pm 13$, $\bar{k} = 4.5$, and $\gamma = 2.5$, averaged over 100 realizations. Inset: data collapse of the rescaled wealth variance in the equilibrium state. (b) Wealth of rich nodes versus degree plus one at different times for $p = 2.5 \times 10^{-6}$ and $\varepsilon = 0.05$ on SF networks with $N = 27989 \pm 27$, $\bar{k} = 4.5$, and $\gamma = 2.5$. (c) Plots of the probability $\rho_{\text{rich}}(k)$ of a node of degree k to be rich. (d) Time-decay of the rich-node density ρ_{rich} in the generalized YS model compared with the random-walker density ρ in the CRW for $(p_1, \varepsilon_1) = (2.0 \times 10^{-6}, 0.1)$ and $(p_2, \varepsilon_2) = (2.5 \times 10^{-6}, 0.05)$ on SF networks with different N 's and \bar{k} 's [26]. The dashed line is Eq. (10). (e) Data collapse of the rescaled wealth variance as predicted in Eq. (11) for $\{(p_1, \varepsilon_1), (p_2, \varepsilon_2)\}$ as in (d) and different N 's, \bar{k} 's and $\gamma = 2.5$. Inset: Wealth variance versus N at fixed time $t = 1.25/\varepsilon p$ with $p = 2.5 \times 10^{-6}$ and $\varepsilon = 0.05$ for two different γ 's. The dashed line has slope $1/3$. (f) The same plots as in (e) for $\gamma = 10$. The dashed lines in (e) and (f) have slope 1.

the wealth of the local rich nodes to their poor neighbors.

Relaxation phase—On the time scale longer than t_{rel} , the RD transfers occur frequently enough to redistribute the locally-concentrated wealth to a neighboring node. Also one of the two local wealths on neighboring nodes can absorb the other [27]. Such coalescence of wealth drives

wealth to a single or a few nodes until the stationary state is reached, and we call this period the *relaxation* phase ($t_{\text{rel}} \lesssim t \lesssim t_{\text{eq}}$).

The wealth variance in this phase exhibits interesting scaling behaviors [Fig. 3]. The dynamics of wealth can be understood by studying the coalescing random walk (CRW) on complex networks [28, 29], which allows us to evaluate $\rho_{\text{rich}}(k)$ and $\omega_{\text{rich}}(k)$, varying with time, and use them in Eq. (8) to obtain the wealth variance. In the CRW suited for our model, the following occurs for every link with rate λ : i) if the link is occupied by a walker (local wealth) at one end node and empty at the other end, the walker moves to the latter, ii) if both end nodes are occupied by walkers, they coalesce leaving one walker at either end node, and iii) if both ends are empty, nothing happens over the link. One can show that the time-decrease of the walker density is proportional to the square of the density and obtain the solution $\rho \simeq \frac{1}{\lambda k t}$. The details are in SM. The jump rate λ is governed by the rate of RD transfers and thus given by $\lambda_{\text{gYS}} \sim \varepsilon p$. Therefore the fraction of rich nodes ρ_{rich} in our model is

$$\rho_{\text{rich}} \simeq \frac{1}{\varepsilon p k t} \quad (10)$$

for large t . It is confirmed by simulations [Figs. 3(d)].

As random movement and coalescence of local wealth proceeds, the probability of a node to be rich $\rho_{\text{rich}}(k)$ loses its dependence on degree k , in contrast to the local condensate phase [Fig. 3(c)]. The wealth of a node remains proportional to its degree [Fig. 3(b)] with the proportional coefficient increasing as the number of rich nodes decreases. Assuming $\omega_{\text{rich}}(k) \simeq c k$ with c a coefficient and $\rho_{\text{rich}}(k) \simeq \rho_{\text{rich}}$ in Eq. (10), one can use the unit mean wealth condition $\bar{\omega} \simeq \sum_k P_{\text{deg}}(k) \rho_{\text{rich}}(k) c k \simeq \rho_{\text{rich}} c \bar{k} = 1$ to obtain $c \simeq \frac{1}{\rho_{\text{rich}} \bar{k}}$. Using these results in Eq. (8), we find

$$\sigma^2(t) \simeq \rho_{\text{rich}} c^2 \bar{k}^2 \sim \begin{cases} \varepsilon p \bar{k} N^{\frac{3-\gamma}{\gamma-1}} t & \text{for } 2 < \gamma < 3, \\ \varepsilon p k t & \text{for } \gamma > 3, \end{cases} \quad (11)$$

where we used $\frac{\bar{k}^n}{k^n} \sim \max\{1, N^{\frac{n-\gamma+1}{\gamma-1}}\}$ for the static-model SF networks [25]. The data collapses of the scaled plots for different ε, p, \bar{k} and N in Fig. 3(e) and 3(f) confirm these distinct scaling behaviors between $2 < \gamma < 3$ and $\gamma > 3$.

The influence of the network structure is remarkable: A large and heterogeneous network (small γ) facilitates wealth condensation by large wealth inequality and small t_{rel} and t_{eq} [26]. Moreover, the correlation of wealth and node degree leads the wealth distribution to share the similar asymptotic behaviors with the degree distribution, $P(\omega) \sim \omega^{-\gamma}$ for large ω while it behaves as $P(\omega) \sim \omega^{-1}$ for small ω [26]. A large ratio p of the RD transfers increases wealth inequality while decreasing the stationary-state wealth variance. The increase of

the fraction ε not only speeds up the whole process, as shown in Eq. (2), but also increases stochasticity and thereby enhances the stationary-state wealth variance as shown in Eq. (4).

Discussions— In this study, we have characterized the scaling properties of wealth inequality, represented by wealth variance, in both its dynamics and steady-state. In the process, we have identified the critical value for redistribution ratio which is inversely proportional to the population size. Furthermore, the evolution of wealth inequality on a sparsely-connected population undergoes multiple phases, revealing the effects of network structure: If heterogeneously connected, a large population progresses into an inequality at a greater rate than a small one, while if homogeneously connected, the population size does not affect the speed much. This is direct consequence of the correlation between wealth and node degree. Our study thus demonstrates that the relevance of the network structure to the wealth distribution in the non-stationary state should be considered in analyzing the real-world wealth inequality.

The real-world income distributions, which we obtain by using the empirical data in Ref. [5, 6], decays slow for small income and then fast for large income with the latter characterized by a power-law with the exponent between 2 and 3 for the past 200 years [26]. Similar features are seen also in the relaxation phase of our model: $P(\omega) \sim \omega^{-1}$ for small ω crossovers to $\sim \omega^{-\gamma}$ for large ω , demanding further investigations with more data. Also the influence of the dimensionality of the underlying network on the speed of wealth condensation deserves further investigation.

We thank Su-Chan Park for helpful discussion. This work was funded by KIAS Individual Grants (CG079901 (D.-S.L) and CG084501 (H.G.L)) at Korea Institute for Advanced Study. We are grateful to the Center for Advanced Computation in KIAS for providing computing resources.

* supersting85@kias.re.kr

† deoksunlee@kias.re.kr

[1] V. Pareto, J. Political Econ. **5**, 485 (1897).

[2] M. Levy and S. Solomon,

Int. J. Mod. Phys. C **07**, 595 (1996).

[3] X. Gabaix, Annu. Rev. Econ. **1**, 255 (2009).

[4] T. Piketty, *Capital in the twenty-first century* (Harvard University Press, Massachusetts, 2017).

[5] L. Chancel and T. Piketty, J. Eur. Econ. Assoc. **19**, 3025 (2021).

[6] L. Chancel, T. Piketty, E. Saez, and G. Zucman, *World inequality report 2022* (Harvard University Press, Massachusetts, 2022).

[7] S. Ispolatov, P. L. Krapivsky, and S. Redner, Eur. Phys. J. B **2**, 267 (1998).

[8] J.-P. Bouchaud and M. Mézard, Physica A **282**, 536 (2000).

[9] A. Dragulescu and V. Yakovenko, Eur. Phys. J. B **17**, 723 (2000).

[10] E. Samanidou, E. Zschischang, D. Stauffer, and T. Lux, Rep. Prog. Phys. **70**, 409 (2007).

[11] V. M. Yakovenko and J. B. Rosser Jr., Rev. Mod. Phys. **81**, 1703 (2009).

[12] M.-Y. Cha, J. W. Lee, and D.-S. Lee, J. Korean Phys. Soc. **56**, 998 (2010).

[13] M. Barbier and D.-S. Lee, J. Stat. Mech. **2017**, 123403 (2017).

[14] A. Chakraborti and B. K. Chakraborti, Eur. Phys. J. B **17**, 167 (2000).

[15] B. Hayes, Am. Sci. **90**, 400 (2002).

[16] B. M. Boghosian, Phys. Rev. E **89**, 042804 (2014).

[17] A. Chakraborti, Int. J. Mod. Phys. C **13**, 1315 (2002).

[18] S. Sinha, Phys. Scr. **2003**, 59 (2003).

[19] C. F. Moukarzel, S. Gonçalves, J. R. Iglesias, M. Rodríguez-Achach, and R. Huerta-Quintanilla, Eur. Phys. J. **143**, 75 (2007).

[20] C. F. Moukarzel, J. Stat. Mech. **2011**, P08023 (2011).

[21] R. Bustos-Guajardo and C. F. Moukarzel, J. Stat. Mech. **2012**, P12009 (2012).

[22] B. M. Boghosian, A. Devitt-Lee, M. Johnson, J. Li, J. A. Marcq, and H. Wang, Physica A **476**, 15 (2017).

[23] A.-L. Barabási and R. Albert, Science **286**, 509 (1999).

[24] K.-I. Goh, B. Kahng, and D. Kim, Phys. Rev. Lett. **87**, 278701 (2001).

[25] D.-S. Lee, K.-I. Goh, B. Kahng, and D. Kim, Nucl. Phys. B **696**, 351 (2004).

[26] See Supplemental Material for derivation of the Langevin equation, the wealth distributions from the Fokker-Planck and Boltzmann equations, the density of random-walkers in the CRW, the phase diagram, and the analysis of the empirical wealth inequality, and supplementary figures.

[27] H. G. Lee, HGL's github repository [URL] for videos showing the simulations of the generalized YS model on SF networks.

[28] M. Catanzaro, M. Boguñá, and R. Pastor-Satorras, Phys. Rev. E **71**, 056104 (2005).

[29] S.-C. Park, Phys. Rev. E **101**, 052125 (2020).

Supplemental Material

Langevin equation for the generalized YS model: Derivation of Eq. (2)

Let us consider the generalized YS model for a network of N nodes and L links with the adjacency matrix A_{ij} . At each time step τ , one selects a pair of connected nodes $s(\tau)$, say (i, j) , among L pairs and performs the YS-mode transfer for the chosen pair if a random variable $g(\tau) = 1$ or the RD-mode transfer if $g(\tau) = 0$. The random variable g is 1 with probability $1 - p$ and 0 with probability p . The node i becomes the sender if another random variable $d(\tau) = -1$, or the node j becomes the sender if $d(\tau) = 1$ with equal probability $\frac{1}{2}$. Given these random variables $s(\tau)$, $g(\tau)$, and $d(\tau)$, the change of the wealth ω_i of a node i for the period from τ_0 to $\tau_0 + \Delta\tau$ is given by

$$\begin{aligned}\Delta\omega_i &\equiv \omega_i(\tau_0 + \Delta\tau) - \omega_i(\tau_0) \\ &= \sum_{\tau'=\tau_0}^{\tau_0+\Delta\tau-1} \sum_{j=1}^N A_{ij} \delta_{s(\tau'), (ij)} \left[\varepsilon g(\tau') \left(\frac{1+d(\tau')}{2} \omega_j - \frac{1-d(\tau')}{2} \omega_i \right) + \varepsilon \{1 - g(\tau')\} d(\tau') \min(\omega_i, \omega_j) \right] \\ &\simeq \varepsilon \sum_{j=1}^N A_{ij} \left[p \frac{\Delta\tau}{L} \frac{\omega_j - \omega_i}{2} + \sqrt{p \frac{\Delta\tau}{L}} \frac{\omega_i + \omega_j}{2} \eta_{ij} + \sqrt{(1-p) \frac{\Delta\tau}{L}} \min(\omega_i, \omega_j) \xi_{ij} \right]\end{aligned}\quad (S1)$$

with the continuous random variables η_{ij} and ξ_{ij} satisfying $\langle \eta_{ij} \rangle = \langle \xi_{ij} \rangle = 0$, $\langle \eta_{ij}^2 \rangle = \langle \xi_{ij}^2 \rangle = 1$, $\eta_{ij} = -\eta_{ji}$, and $\xi_{ij} = -\xi_{ji}$. Introducing time $t \equiv \frac{\tau}{N}$ and taking large- N limit, we find

$$d\omega_i = -\frac{\varepsilon p}{k} \sum_j L_{ij} \omega_j dt + \varepsilon \sqrt{\frac{2p}{k}} \sum_j A_{ij} \frac{\omega_i + \omega_j}{2} dC_{ij} + \varepsilon \sqrt{\frac{2(1-p)}{k}} \sum_j A_{ij} \min(\omega_i, \omega_j) dB_{ij} \quad (S2)$$

where dB_{ij} and dC_{ij} are the Wiener processes satisfying $\langle dB_{ij} \rangle = \langle dC_{ij} \rangle = 0$, $\langle dB_{ij}^2 \rangle = \langle dC_{ij}^2 \rangle = dt$, $dB_{ij} = -dB_{ji}$, and $dC_{ij} = -dC_{ji}$. To fulfill the condition $\sum_i d\omega_i = 0$, we adopted the Itô's scheme. To proceed, we approximate the sum of the YS- and RD-mode transfers with all the nearest neighbors as

$$\begin{aligned}\sqrt{\frac{1}{k}} \sum_j A_{ij} \frac{\omega_i + \omega_j}{2} dC_{ij} &\simeq \sqrt{D^{(\text{RD})}(\omega_i)} dX_i \quad \text{and} \\ \sqrt{\frac{1}{k}} \sum_j A_{ij} \min(\omega_i, \omega_j) dB_{ij} &\simeq \sqrt{D^{(\text{YS})}(\omega_i)} dY_i,\end{aligned}\quad (S3)$$

where dX_i and dY_i are the Wiener processes satisfying $\langle dX_i \rangle = \langle dY_i \rangle = 0$, $\langle dX_i^2 \rangle = \langle dY_i^2 \rangle = dt$. The coefficients $D^{(\text{RD})}(\omega)$ and $D^{(\text{YS})}(\omega)$ are given by

$$\begin{aligned}D^{(\text{RD})}(\omega_i) &= \left\langle \frac{1}{k} \sum_{j=1}^N A_{ij} \left(\frac{\omega_i + \omega_j}{2} \right)^2 \right\rangle \simeq \left\langle \frac{1}{N} \sum_{j=1}^N \left(\frac{\omega_i + \omega_j}{2} \right)^2 \right\rangle, \\ D^{(\text{YS})}(\omega_i) &= \left\langle \sum_{j=1}^N A_{ij} [\min\{\omega_i, \omega_j\}]^2 \right\rangle \simeq \left\langle \frac{1}{N} \sum_{j=1}^N [\min\{\omega_i, \omega_j\}]^2 \right\rangle\end{aligned}$$

with $\langle \dots \rangle$ representing the ensemble average. While these coefficients are not expressed in the closed form [16], we find its limiting behaviors given by

$$\begin{aligned}D^{(\text{RD})}(\omega) &\simeq \begin{cases} \frac{\langle \omega^2 \rangle}{4} & \text{for } \omega \rightarrow 0, \\ \frac{\omega^2}{4} & \text{for } \omega \rightarrow \infty, \end{cases} \\ D^{(\text{YS})}(\omega) &\simeq \begin{cases} \omega^2 & \text{for } \omega \rightarrow 0, \\ \langle \omega^2 \rangle & \text{for } \omega \rightarrow \infty \end{cases}\end{aligned}\quad (S4)$$

with $\bar{x} = N^{-1} \sum_j x_j$ the spatial average. Also note that $D^{(\text{RD})}(\omega) \simeq 1$ and $D^{(\text{YS})}(\omega) \simeq 1$ for ω close to the initial value 1 in the early-time regime when all nodes have wealth close to 1.

Wealth distribution for small p : Derivation of Eqs. (5) and (6)

Consider for sufficiently small p the early time-regime when $\omega_i(t)$ is not much different from the initial value $\omega_i(0) = 1$. Then, Eq. (2) in the main text is approximated as

$$d\omega_i = \varepsilon \sqrt{2D^{(\text{YS})}(\omega_i)} dY_i, \quad (\text{S5})$$

and the corresponding Fokker-Planck equation is given by

$$\frac{\partial}{\partial t} P(\omega, t) = \varepsilon^2 \frac{\partial^2}{\partial^2 \omega} \left(D_{\text{YS}}(\omega) P(\omega, t) \right). \quad (\text{S6})$$

For $\omega \ll \bar{\omega} = 1$, the coefficient $D^{(\text{YS})}(\omega)$ in Eq. (S4) can be approximated by $D_{\text{YS}}(\omega) \simeq \omega^2$, which is inserted into Eq. (S6) to yield

$$P(\omega, t) \simeq \frac{e^{-t\varepsilon^2/4}}{\sqrt{4\pi\varepsilon^2 t}} \frac{1}{\omega^{3/2}} \exp \left[-\frac{(\log \omega)^2}{4\varepsilon^2 t} \right] \quad (\text{S7})$$

as in Eq. (5). On the other hand, if $\omega \gg \bar{\omega} = 1$, we find $D^{(\text{YS})}(\omega) \simeq \langle \omega^2 \rangle \simeq 1$, and the corresponding Fokker-Planck equation $(\partial/\partial t)P = \varepsilon^2(\partial^2/\partial \omega^2)P$ will give the Gaussian distribution as the solution:

$$P(\omega, t) \simeq \frac{1}{\sqrt{4\pi\varepsilon^2 t}} e^{-\frac{(\omega-1)^2}{4\varepsilon^2 t}} \quad (\text{S8})$$

as in Eq. (6).

In the long-time limit, the approximations that we take as in the above for the left or right tail only are not working but one should refer to the Boltzmann equation [16]

$$\begin{aligned} \frac{\partial P(\omega, t)}{\partial t} = & - \left[P(\omega, t) - \frac{1}{1+\varepsilon} P\left(\frac{\omega}{1+\varepsilon}, t\right) \right] - \left[P(\omega, t) - \frac{1}{1-\varepsilon} P\left(\frac{\omega}{1-\varepsilon}, t\right) \right] \\ & + \int_0^{\frac{\omega}{1+\varepsilon}} d\omega' \left[P(\omega - \varepsilon\omega', t) - \frac{1}{1+\varepsilon} P\left(\frac{\omega}{1+\varepsilon}, t\right) \right] P(\omega', t) \\ & + \int_0^{\frac{\omega}{1-\varepsilon}} d\omega' \left[P(\omega + \varepsilon\omega', t) - \frac{1}{1-\varepsilon} P\left(\frac{\omega}{1-\varepsilon}, t\right) \right] P(\omega', t) \end{aligned} \quad (\text{S9})$$

under the random-agent approximation. Then, one can find the following solution by direct substitution:

$$P(\omega, t) = \frac{C}{\omega(t + t_0)} \quad (\text{S10})$$

with t_0 a finite constant and C given by

$$C = \frac{1}{\log\left(\frac{1}{1-\varepsilon^2}\right)}. \quad (\text{S11})$$

Wealth distribution for large p : Derivation of Eq. (7)

When p is large but sufficiently smaller than 1, one can approximate Eq. (2) in the main text by keeping the leading terms of order dt and \sqrt{dt} as

$$d\omega_i \simeq -\varepsilon p \frac{k_i}{k} (\omega_i - \bar{\omega}) dt + \varepsilon \sqrt{2(1-p)D^{(\text{YS})}(\omega_i)} dY_i. \quad (\text{S12})$$

The Fokker-Planck equation is then given by

$$\frac{\partial P(\omega, t)}{\partial t} = \frac{\partial}{\partial \omega} \left\{ \varepsilon p (\omega - 1) P(\omega, t) \right\} + \frac{1}{2} \frac{\partial^2}{\partial^2 \omega} \left\{ 2\varepsilon^2 (1-p) D^{(\text{YS})}(\omega) P(\omega, t) \right\}, \quad (\text{S13})$$

where we assumed $\frac{k_i}{k} \simeq 1$ as a mean-field approximation. In the equilibrium state where $\frac{\partial P}{\partial t} = 0$, the wealth distribution $P_{\text{eq}}(\omega)$ in the small- ω regime, where $D^{(\text{YS})}(\omega) \simeq \omega^2$ as in Eq. (S4), satisfies

$$\mu(\omega - 1)P_{\text{eq}} + \frac{\partial}{\partial \omega}(\omega^2 P_{\text{eq}}) = 0 \quad (\text{S14})$$

with $\mu \equiv \frac{p}{\varepsilon(1-p)}$, the solution of which is given by [8]

$$P_{\text{eq}}(\omega) = \frac{\mu^{\mu+1}}{\Gamma(\mu+1)} \omega^{-\mu-2} e^{-\frac{\mu}{\omega}} \quad (\text{S15})$$

as in Eq. (7). The mean and variance of Eq. (S15) are given by

$$\langle \omega \rangle = 1 \quad \text{and} \quad \langle \omega^2 \rangle - \langle \omega \rangle^2 = \frac{1}{\mu - 1}, \quad (\text{S16})$$

if $\mu > 1$. One can see that $\langle \omega^2 \rangle - \langle \omega \rangle^2 \simeq \frac{1}{\mu} \simeq \frac{\varepsilon}{p}$ if $\varepsilon \ll p$.

Density of random-walkers in the CRW: Derivation of Eq. (10)

Following [28], we can see that the number of random-walkers, $n_i = 0$ or 1 , on node i at time $t + dt$ in the CRW model is given by

$$n_i(t + dt) = n_i(t)\eta + (1 - n_i(t))\xi \quad (\text{S17})$$

with

$$\eta = \begin{cases} 0 & \text{with probability } \lambda dt \sum_j a_{ij}(1 - n_j) + \lambda dt \sum_j a_{ij}n_j, \\ 1 & \text{otherwise,} \end{cases} \quad (\text{S18})$$

and

$$\xi = \begin{cases} 1 & \text{with probability } \lambda dt \sum_j a_{ij}n_j, \\ 0 & \text{otherwise.} \end{cases} \quad (\text{S19})$$

Here, $\eta = 0$ represents the disappearance of the random-walker at node i because of a jump to a nearest node (with probability $\lambda dt \sum_j a_{ij}(1 - n_j)$), or coalescence to a neighbor node (with probability $\lambda dt \sum_j a_{ij}n_j$). On the other hand, $\xi = 1$ represents the arrival of a walker at node i from a neighbor node (with probability $\lambda dt \sum_j a_{ij}n_j$). Taking the ensemble average for a given $n_i(t)$, we have

$$\langle n_i(t + dt) \rangle = n_i(t)(1 - \lambda dt \sum_j a_{ij}) + (1 - n_i(t))\lambda dt \sum_j a_{ij}n_j(t), \quad (\text{S20})$$

which leads to

$$\frac{d\rho_i}{dt} = -\lambda k_i \rho_i + \lambda(1 - \rho_i) \sum_j a_{ij} \rho_j, \quad (\text{S21})$$

where the density of random-walker is denoted by $\rho_i = \langle n_i \rangle$ and the independence of ρ_i and ρ_j for $i \neq j$ is assumed. Assuming that ρ_i at node i is a function of its degree k_i and equivalently $\rho_i = \rho_j$ if $k_i = k_j$, we can rewrite Eq. (S21) as

$$\frac{d\rho_k}{dt} = -\lambda k \rho_k + \lambda k(1 - \rho_k) \sum_{k'} \frac{k' P_{\text{deg}}(k')}{\bar{k}} \rho_{k'}, \quad (\text{S22})$$

where $\rho_k \equiv \frac{1}{N} \sum_{i=1}^N \delta_{k_i, k} \rho_i$ and $P_{\text{deg}}(k)$ is the degree distribution of the underlying network. Note that $\rho = \sum_k P_{\text{deg}}(k) \rho_k$. Let us also introduce $\tilde{\rho} \equiv \sum_k \frac{k P_{\text{deg}}(k)}{\bar{k}} \rho_k$. Multiplying Eq. (S22) by $P_{\text{deg}}(k)$ and summing over k , we find

$$\frac{d\rho}{dt} = -\lambda \bar{k} \tilde{\rho} + \lambda \bar{k} \tilde{\rho}(1 - \tilde{\rho}) = -\lambda \bar{k} \tilde{\rho}^2. \quad (\text{S23})$$

In the long-time limit, we expect $\frac{d\rho_k}{dt}$ is much smaller than ρ_k or $\tilde{\rho}$ in Eq. (S22), so we assume that the right-hand-side of Eq. (S22) is zero, to obtain

$$\rho_k \simeq \frac{\tilde{\rho}}{1 + \tilde{\rho}}, \quad (\text{S24})$$

which means that ρ_k is independent of k . This also implies that

$$\rho = \sum_k P_{\text{deg}}(k) \rho_k = \frac{\tilde{\rho}}{1 + \tilde{\rho}} \quad \text{or} \quad \tilde{\rho} = \frac{\rho}{1 - \rho}. \quad (\text{S25})$$

Inserting Eq. (S25) into Eq. (S23), we have

$$\frac{d\rho}{dt} = -\lambda \bar{k} \left(\frac{\rho}{1 - \rho} \right)^2 \simeq -\lambda \bar{k} \rho^2, \quad (\text{S26})$$

where the last relation holds for $\rho \ll 1$ which will be valid in the long-time limit. Therefore, from Eq. (S26), we have

$$\rho \simeq \frac{1}{\lambda \bar{k} t} \quad (\text{S27})$$

which gives $\rho_{\text{rich}} \sim \rho \sim \frac{1}{\varepsilon p \bar{k} t}$ with $\lambda_{gYS} = \varepsilon p$ as in Eq. (10) in the main text. It takes $t_{\text{hop}} \sim \frac{1}{\varepsilon p}$ for the local wealth at a rich node i to be fully redistributed to its poor neighbors and itself, which is understood by considering $\frac{\varepsilon p}{\bar{k}} k_i (\omega_i - 1) t_{\text{hop}} \sim \omega_i - 1$ and essentially determines the rate $\lambda_{gYS} \simeq \frac{1}{t_{\text{hop}}} \sim \varepsilon p$ of random hopping of local wealth.

Phase diagram

In this section, we collect all the different behaviors of the wealth variance depending on the model parameters and the structure of the underlying networks as studied in the main text to provide an overview of the multiple phases in the time-evolution of wealth inequality on sparse networks. From Eqs. (3), (4), (9), and (11), we obtain

$$\sigma^2(t) \sim \begin{cases} \varepsilon^2 t & \text{for } t \ll t_{\text{lc}}, \\ \bar{k} & \text{for } t_{\text{lc}} \ll t \ll t_{\text{rel}}, \\ \bar{k} \varepsilon p t \max\{1, N^{\frac{3-\gamma}{\gamma-1}}\} & \text{for } t_{\text{rel}} \ll t \ll t_{\text{eq}}, \\ \min\{N, \frac{\varepsilon}{p}\} & \text{for } t \gg t_{\text{eq}} \end{cases} \quad (\text{S28})$$

which reveals the early-time growth, local condensate, relaxation phase before the stationary state. The crossover time scales are given by

$$\begin{aligned} t_{\text{lc}} &= \frac{\bar{k}}{\varepsilon^2}, \\ t_{\text{rel}} &= \frac{1}{\varepsilon p \max\{1, N^{\frac{3-\gamma}{\gamma-1}}\}} = \begin{cases} t_{\text{rel}}^{(\text{het})} = \frac{1}{\varepsilon p N^{\frac{3-\gamma}{\gamma-1}}} & \text{for } 2 < \gamma < 3, \\ t_{\text{eq}}^{(\text{hom})} = \frac{1}{\varepsilon p} & \text{for } \gamma > 3, \end{cases} \\ t_{\text{eq}} &= \frac{\min\{N, \frac{\varepsilon}{p}\}}{\bar{k} \varepsilon p t \max\{1, N^{\frac{3-\gamma}{\gamma-1}}\}} = \begin{cases} t_{\text{eq,C}}^{(\text{het})} = \frac{N^{\frac{2(\gamma-2)}{\gamma-1}}}{\varepsilon p \bar{k}} & \text{for } p \ll p_*, 2 < \gamma < 3, \\ t_{\text{eq,F}}^{(\text{het})} = \frac{1}{p^2 \bar{k} N^{\frac{3-\gamma}{\gamma-1}}} & \text{for } p \gg p_*, 2 < \gamma < 3, \\ t_{\text{eq,C}}^{(\text{hom})} = \frac{N}{\varepsilon p \bar{k}} & \text{for } p \ll p_*, \gamma > 3, \\ t_{\text{eq,F}}^{(\text{hom})} = \frac{1}{p^2 \bar{k}} & \text{for } p \gg p_*, \gamma > 3, \end{cases} \end{aligned} \quad (\text{S29})$$

and the criterion between the global condensate phase and fluid phase given by $p_* \equiv \frac{\varepsilon}{N}$. We remark that on the complete graphs ($\bar{k} = N - 1$), the local condensate phase in Eq. (S28) is identical to the global condensate phase $\sigma^2 \simeq N$ and therefore t_{lc} in Eq. (S29) should be considered as the equilibration time.

The scaled plots in Fig. 3 (e) and (f) confirm the crossover around t_{rel} for $p \ll p_*$. The crossover around the equilibration time is shown in the data collapse of the scaled plots in Fig. S4. From Eqs. (S28) and (S29), we can obtain the diagram of different phases as in Fig. S5(a) and S5(b) for $2 < \gamma < 3$ and $\gamma > 3$, respectively.

Wealth distribution in the real world in 1820 - 2020 and our model

We use two data-sets of the world income distribution, one in Ref. [5] covering a few selected years in the period 1820 to 2020 and the other in Ref. [6] providing annual data from 1980 to 2016. Both data-sets provide for each given year the average income $W(x)$ of the people who belong to the top x % of the whole population in the world regarding their income with $x = 0.01, 0.1, 1, 10, 50$, and 100 . We can consider 6 distinct groups of people according to their income: bottom 50%, top 50% to top 10%, top 10% to top 1%, top 1% to top 0.1%, top 0.1% to top 0.01%, and the top 0.01%. The average incomes of the people in these 6 distinct groups and their portions are then given by

$$\begin{cases} W_1 = W(100) - W(50), & f_1 = 0.5, \\ W_2 = W(50) - W(10), & f_2 = 0.4, \\ W_3 = W(10) - W(1), & f_3 = 0.09, \\ W_4 = W(1) - W(0.1), & f_4 = 0.009, \\ W_5 = W(0.1) - W(0.01), & f_5 = 0.0009, \\ W_6 = W(0.01), & f_6 = 0.0001. \end{cases} \quad (\text{S30})$$

Notice that $\sum_{\ell=1}^6 f_i = 1$. We can use these values to compute the mean wealth

$$\overline{W} = \sum_{\ell=1}^6 W_{\ell} f_{\ell}. \quad (\text{S31})$$

To compare the properties of these real-world incomes with the wealth considered in the main text, we consider the rescaled income

$$\omega_{\ell} = \frac{W_{\ell}}{\overline{W}} \quad (\text{S32})$$

for $\ell = 1, 2, 3, 4, 5, 6$. The income variance is then evaluated as

$$\sigma^2 = \sum_{\ell=1}^6 \omega_{\ell}^2 f_{\ell} - 1 \quad (\text{S33})$$

and the (rescaled) income distribution $P(\omega)$ is obtained by

$$p(\omega_{\ell}) = \frac{f_{\ell}}{\Delta\omega_{\ell}}, \quad (\text{S34})$$

where the bin sizes are evaluated as $\Delta\omega_{\ell} = \sqrt{\omega_{\ell}\omega_{\ell+1}} - \sqrt{\omega_{\ell}\omega_{\ell-1}}$ with $\omega_0 = \frac{\omega_1^2}{\sqrt{\omega_1\omega_2}}$ and $\omega_7 = \frac{\omega_6^2}{\sqrt{\omega_5\omega_6}}$. We also compute the Gini index by

$$G = \frac{1}{2} \sum_{\ell_1=1}^6 \sum_{\ell_2=1}^6 |\omega_{\ell_1} - \omega_{\ell_2}| f_{\ell_1} f_{\ell_2}. \quad (\text{S35})$$

where we used $\overline{\omega} = 1$. Note that the wealth variance σ^2 is represented by $\sigma^2 = (1/2) \sum_{\ell_1, \ell_2} (\omega_{\ell_1} - \omega_{\ell_2})^2 f_{\ell_1} f_{\ell_2}$.

The results are shown in Fig. S6(a) and (b). In (c), we show the wealth distributions obtained from our model on SF networks, which are comparable to the former. Here we present the details of the wealth distribution from our model. With a low ratio of the RD-mode transfers ($p \ll p_*$), the wealth distribution in the stationary state takes a power-law with exponent one and almost all wealth goes to a single individual as in the original YS model ($\sigma_{\text{eq}}^2 \simeq N$ as shown in Fig. 3(a)). In the non-stationary state, the poor nodes' wealth, much smaller than the average $\omega \ll \overline{\omega} = 1$, is found to be distributed by the same power-law with exponent one. However, the distributions of rich nodes' wealth (the wealth distribution in the right tail) in the non-stationary state are different, displaying larger power-law exponents than one as shown in Fig. S6(c). Therefore they show a crossover from a slow decay to a fast decay, which is observed also in the real-world wealth distribution in Fig. S6(b).

The fast decay of our model's wealth distributions, describing the wealth of rich nodes, originates in the correlation of wealth with node degree. As we have shown in the main text, the wealth of a rich node is proportional to its degree as

$$\omega_{\text{rich}}(k) \sim c k, \quad (\text{S36})$$

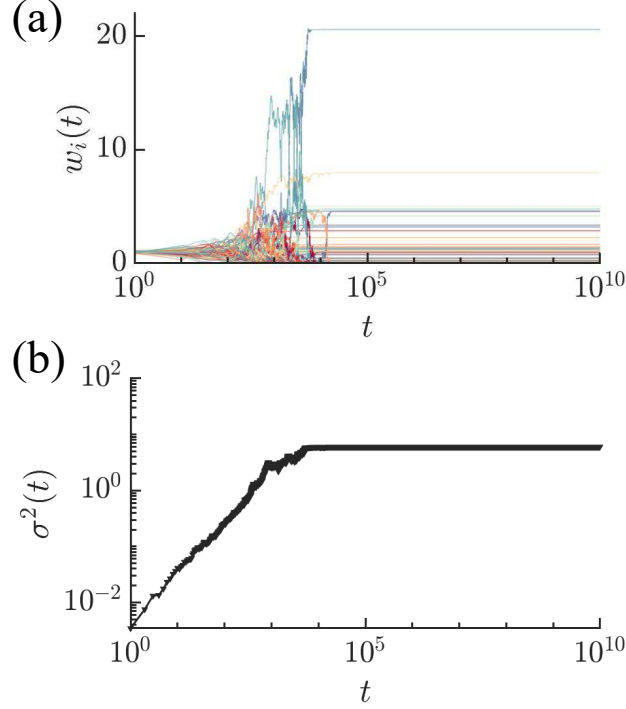


Figure S1. Time evolution of (a) individual wealth ω_i and (b) wealth variance σ^2 in the Monte-Carlo simulation of the generalized YS model with $p = 0$ on the same SF network as in Fig. 1.

where the coefficient c is close to one in the local condensation phase and $c \simeq \varepsilon p t$ in the relaxation phase. Also, the probability of a node to be rich is given by

$$\rho_{\text{rich}}(k) \simeq \begin{cases} \frac{1}{k+1} & \text{for } t_{\text{lc}} \ll t \ll t_{\text{rel}}, \\ \rho_{\text{rich}} & \text{for } t_{\text{rel}} \ll t \ll t_{\text{eq}}, \end{cases} \quad (\text{S37})$$

in the local condensation and relaxation phase, respectively, with ρ_{rich} given in Eq. (10). Therefore the wealth distribution $P(\omega)$ for large ω is evaluated by using the degree distribution $P_{\text{deg}}(k)$ as

$$\begin{aligned} P(\omega) &\sim \sum_k P_{\text{deg}}(k) \rho_{\text{rich}}(k) \delta(\omega_{\text{rich}}(k) - \omega) \sim P_{\text{deg}}\left(k \simeq \frac{\omega}{c}\right) \rho_{\text{rich}}\left(k \simeq \frac{\omega}{c}\right) \\ &\sim \begin{cases} \omega^{-\gamma-1} & \text{for } t_{\text{lc}} \ll t \ll t_{\text{rel}}, \\ \omega^{-\gamma} & \text{for } t_{\text{rel}} \ll t \ll t_{\text{eq}}. \end{cases} \end{aligned} \quad (\text{S38})$$

This means that the power-law exponent of the wealth distribution $P(\omega)$ for large ω may change from $\gamma + 1$ to γ . In the relaxation phase, the number of rich nodes decreases [Eq. (10)] and therefore the fast-decaying region shrinks and eventually disappears in the stationary state, in which the power-law distribution with exponent one describes the wealth distribution. In Fig. S6(c), we present the wealth distributions obtained on the SF networks with $\gamma = 2.5$ at times selected in the local condensate and relaxation phase, which show the variation of the power-law exponent in the large- ω region with time. The overall shape of the wealth distribution looks similar to the real-world wealth distribution in Fig. S6(b).

Our study thus suggests the possibility of the correlation between the wealth distribution and the network structure of the population, emerging from the microscopic correlations like Eqs. (S36) and (S37). It is highly desirable that these predictions be scrutinized by using the empirical data-sets of higher resolution than the ones considered here, e.g., involving the individual's wealth and their metadata particularly about their connectivity.

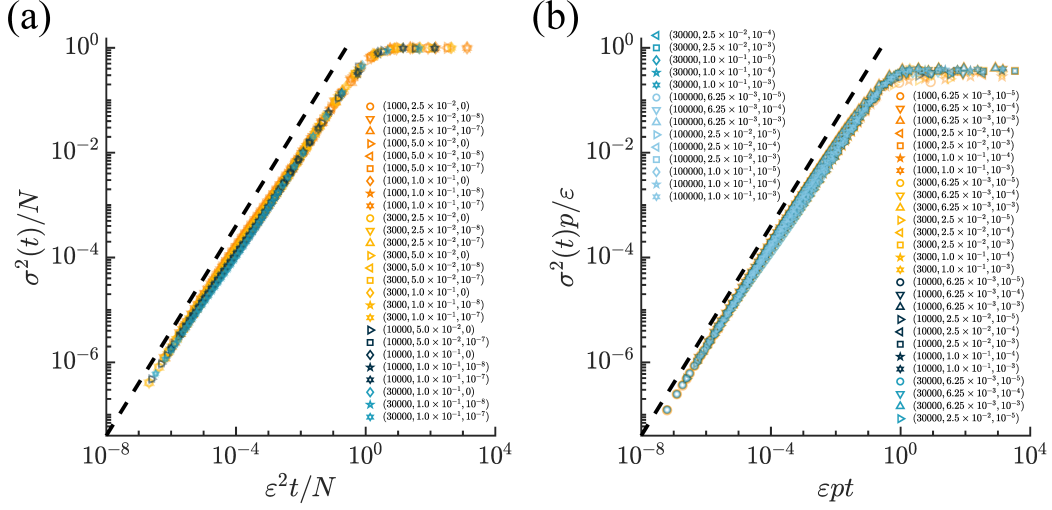


Figure S2. Data collapse of the rescaled wealth variance on the complete graphs with different parameters. Legends specify values for (N, ε, p) . (a) Plots of σ^2/N versus $\varepsilon^2 t/N$ for the parameters satisfying $p < 0.1p_*$ with $p_* \equiv \frac{\varepsilon}{N}$. (b) Plot of $\sigma^2 p/\varepsilon$ versus $\varepsilon p t$ for the parameters satisfying $p > p_*$. Both (a) and (b) can be represented by $\sigma^2(t) = \sigma_{\text{eq}}^2 \Phi\left(\frac{t}{t_{\text{eq}}}\right)$ with the function $\Phi(x) \simeq x$ for $x \ll 1$ and $\Phi(x) \simeq 1$ for $x \gg 1$ and σ_{eq}^2 given in Eq. (4) and the equilibration time given by $t_{\text{eq}} = \frac{N}{\varepsilon^2}$ for $p \ll p_*$ and $t_{\text{eq}} = \frac{1}{\varepsilon p}$ for $p \gg p_*$. The dashed lines are of slope 1.

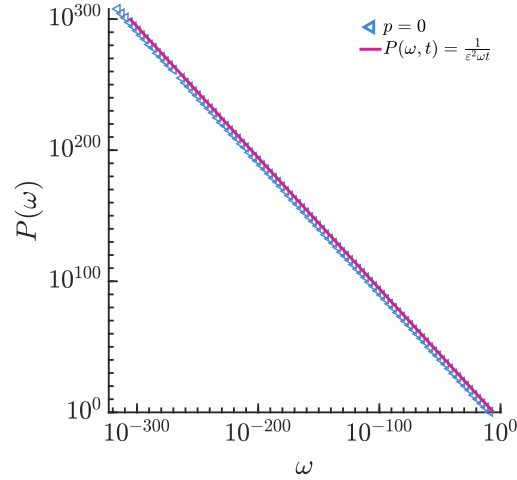


Figure S3. Wealth distribution with $p = 0$ on the complete graphs of $N = 10^5$, $\varepsilon = 0.1$ at time $t = 10^8$.

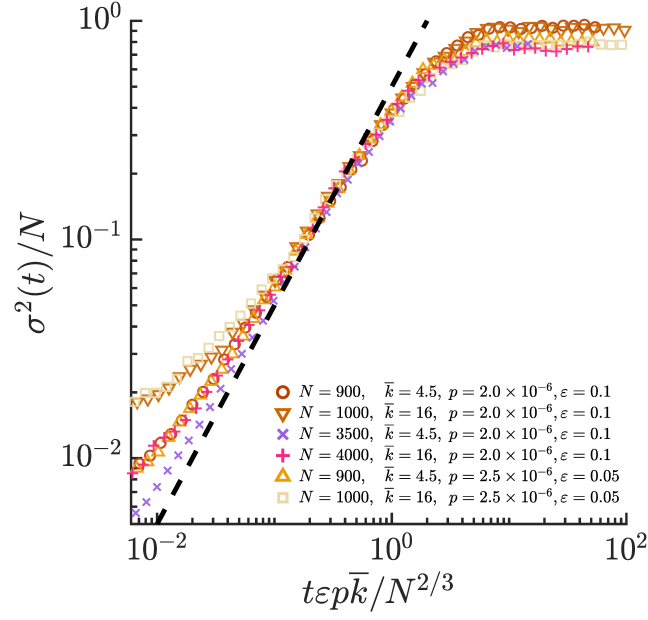


Figure S4. Data collapse of the rescaled wealth variance exhibiting crossover from the relaxation phase to the global condensate phase around $t_{eq} = \frac{N^{2/3}}{\epsilon p \bar{k}}$ with $p < 0.1p_*$ on the SF networks with the degree exponent $\gamma = 2.5$.

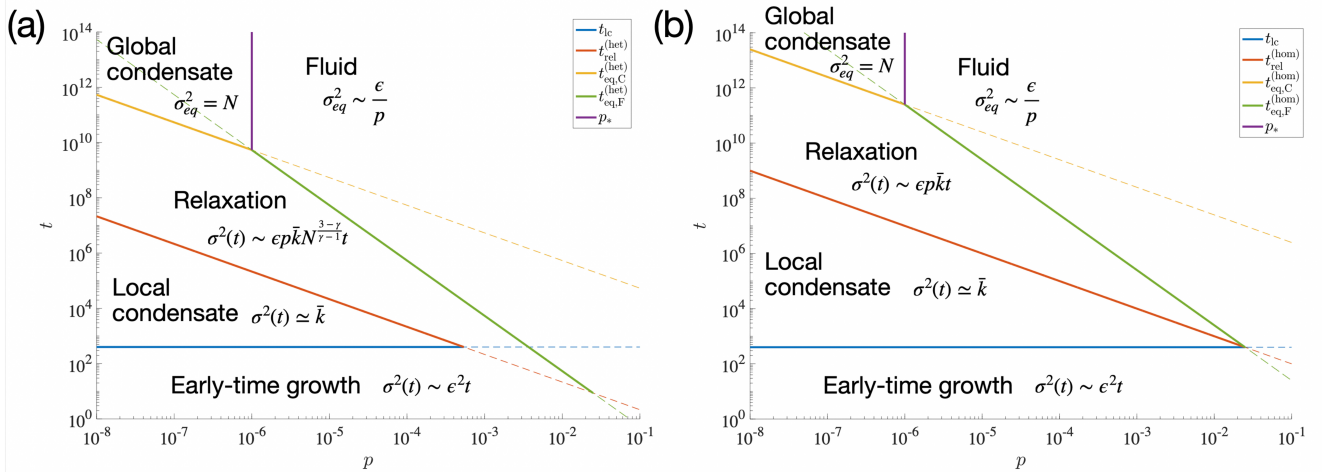


Figure S5. Phase diagram of wealth inequality in the (p, t) plane for the generalized YS model with $\epsilon = 0.1$ on SF networks of $N = 10^5$, $\bar{k} = 4$ and (a) $\gamma = 2.5$ and (b) $\gamma = 10$. The phase boundaries are given by Eq. (S29).

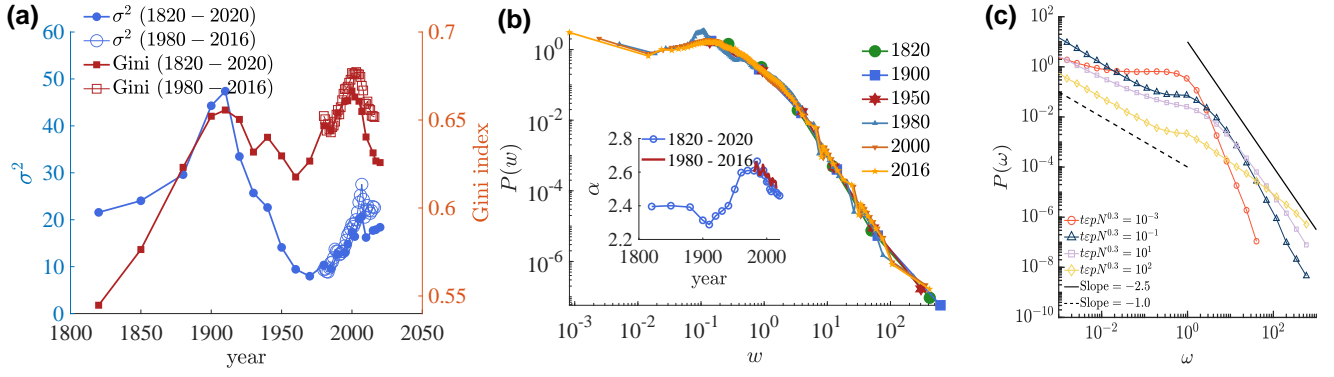


Figure S6. Real-world inequality. (a) Wealth variance σ^2 and the Gini index of the rescaled income in the period 1820 to 2020 (filled points) [5] and in the period 1980 to 2016 (open) [6]. (b) Wealth distributions in 1820, 1900, and 1950 estimated from the data-sets in Ref. [5] and 1980, 2000, and 2016 from Ref. [6]. Inset: The power-law exponent α in $P(\omega) \sim \omega^{-\alpha}$ fitted to the data-sets for $\omega > 10$. (c) Wealth distributions in the generalized YS model with $p = 2.5 \times 10^{-6}$, $\varepsilon = 0.05$ at different times on SF networks with $N = 16000$, $\bar{k} = 16$ and $\gamma = 2.5$. The solid and dashed lines are guide lines with different slopes.